Int. J. Heat Mass Transfer. Vol. 17, pp. 407–419. Pergamon Press 1974. Printed in Great Britain

IMPLICATIONS CONCERNING ROD BUNDLE CROSSFLOW MIXING BASED ON MEASUREMENTS OF TURBULENT FLOW STRUCTURE†

D. S. ROWE and B. M. JOHNSON
Battelle-Northwest Laboratories, Richland, Washington, U.S.A.

and

J. G. KNUDSEN
Oregon State University, Corvallis, Oregon, U.S.A.

(*Received* 7 *May* 1973 *and in revised form* 18 *July* 1973)

Abstract—An experimental study was performed to investigate the effect of flow channel geometry on fully developed turbulent flow in "clean" rod bundle flow channels. This information was sought to obtain a better understanding of crossflow mixing between rod bundle subchannels. The experiments were performed in water with a Reynolds number range from 50 000 to 200 000. The experimental flow models considered pitch-to-diameter ratios of 1·25 and 1·125. Axial components of velocity, turbulence intensity and Eulerian autocorrelation function were the primary measurements. The autocorrelation function provided an indication of the dominant frequency of turbulence and an estimate of the longitudinal macroscale by using Taylor's hypothesis. A limited amount of lateral component turbulence intensity data was also obtained.

The experimental results show that rod gap spacing (pitch-to-diameter ratio) is the most significant geometric parameter affecting the flow structure. Decreasing the rod gap spacing increases the turbulence intensity, longitudinal macroscale, and the dominant frequency of turbulence. These turbulence parameters are rather insensitive to Reynolds number.

The results indicate that macroscopic flow processes exist adjacent to the rod gap. This includes secondary flows and increased scale and frequency of flow pulsations when the rod gap spacing is reduced. When interpreted in terms of crossflow mixing, the results are consistent with present crossflow mixing correlations.

NOMENCLATURE

A, flow area;
d, rod diameter;
D, hydraulic diameter ($4A/P_w$);
f, Darcy friction factor;
f_D, Doppler frequency;
G, mass flux, ρu;
L, mixing length;
n, refractive index;
p, rod pitch;
P_w, wetted perimeter;
r, radial distance;
r_0, reference unit vector;
r_s, scattering unit vector;
Re, Reynolds number (GD/μ);
$R_E(\tau)$, Eulerian correlation function;
$R_L(\tau)$, Lagrangian correlation function;
s, rod gap spacing;
t, time;
T_E, Eulerian time macroscale;
T_L, Lagrangian time macroscale;
U, channel average velocity;
U^*, shear velocity based on U;
u, v, instantaneous velocity components in the x and y direction;
u', v', fluctuating velocity components in the x and y direction;
$\bar{u}$, mean velocity component in the x direction;
V', macroscopic velocity fluctuation;
V, velocity vector;
w', turbulent crossflow per unit length;
x, y, z, Cartesian coordinates;
y, distance from wall;
$\hat{y}$, distance from wall to line of maximum velocity;
α_1, α_2, function fit parameters;
γ, fluctuating component of scalar;
Γ, scalar quantity;
$\bar{\Gamma}$, average value of scalar quantity;
Δy, centroid or "mixing" distance between subchannels;

†This paper is based on work performed under United States Atomic Energy Commission Contract AT(45-1)-1830. Permission to publish is gratefully acknowledged.

ε, eddy diffusivity;
θ, scattering angle;
λ_0, *in vacuo* wavelength of laser light ($\lambda_0 = 6328$ Å, He–Ne);
Λ, Eulerian longitudinal space macroscale as estimated by Taylor's hypothesis;
Λ_f, Eulerian longitudinal space macroscale;
Λ_L, Lagrangian space macroscale;
μ, absolute viscosity;
ρ, density;
τ, time delay;
ϕ, angular coordinate.

INTRODUCTION

THE OBJECTIVE of this paper is to present the results of an experimental study of turbulent flow structure in rod-bundle subchannels as measured by a laser–Doppler velocimeter. The motivation to obtain this information is to improve the understanding of turbulent crossflow mixing processes in rod bundles.

Rod-bundle flow channels form the basic flow configuration for present day fuel designs used in water cooled nuclear power reactors. The thermal-hydraulic performance of rod-bundles is related to the turbulent flow structure through the process of crossflow mixing, since this mixing provides a mechanism to equalize coolant temperatures.

The usual "lumped-parameter" analysis [1–4] of a rod-bundle considers the bundle to be a continuously interconnected set of parallel flow subchannels that are coupled to each other by crossflow mixing. The crossflow mixing, however, is described empirically because a definitive correlating equation for crossflow mixing has not been developed. Several correlations exist, [2, 5–8] but none have been proven to apply generally to all rod-bundle geometries. The lack of a universal correlation, if there is one, is hampered by the incomplete description of turbulent flow structure in rod-bundles and how it is affected by the bundle geometry. Flow processes from simple channels such as round tubes are often extrapolated to rod bundles with only partial success [2].

ROD-BUNDLE MIXING PROCESSES

Turbulent transport of a scalar quantity is expressed as an eddy diffusion process [9] defined by

$$\rho \overline{v'\gamma} = \varepsilon\rho \frac{\partial \bar{\Gamma}}{\partial y}. \tag{1}$$

For the rod bundle analysis [2] a difference approximation to the right side of equation (1), applied to an increment of length is

$$\varepsilon\rho \frac{\partial \bar{\Gamma}}{\partial y}(s\Delta x) \simeq \varepsilon\rho s \frac{\Delta \bar{\Gamma}}{\Delta y}\Delta x. \tag{2}$$

The quantity $\varepsilon\rho s/\Delta y \equiv w'$ is the turbulent crossflow mixing rate per unit length. w' can be expressed in the dimensionless form

$$\frac{w'}{GD} = \left(\frac{\varepsilon}{UD}\right)\left(\frac{s}{\Delta y}\right). \tag{3}$$

This dimensionless equation gives the mixing parameter (w'/GD) in terms of the inverse turbulent Peclet number (ε/UD) and a geometric ratio parameter ($s/\Delta y$). The group w'/GD has been called the mixing Stanton number based on hydraulic diameter. Some correlations [2] use gap spacing for this dimension which gives an alternate form

$$\frac{w'}{Gs} = \left(\frac{\varepsilon}{UD}\right)\left(\frac{D}{\Delta y}\right). \tag{4}$$

Early investigators assumed that the right side of equation (4) was nearly constant or weakly dependent upon Reynolds number with the implication that w' was proportional to gap spacing. A rather large body of experimental data [2, 5–8, 10–13] has now been gathered to show that this is not the case. Instead, the right side of equation (3) is weakly dependent upon rod gap spacing for sufficiently large gap spacings.

Although present experimental evidence indicates a weak dependence of turbulent crossflow mixing rate with gap spacing, a satisfactory explanation of this phenomena has not been developed. The generally accepted explanation is that some additional phenomena, such as macroscopic flow processes or secondary flow, is responsible for the observed behavior [12, 13]. Another is that the scale of turbulence involved in the mixing processes is essentially proportional to gap spacing [8] for $s/d > 0{\cdot}1$. Ibragimov *et al.* [14], in their theoretical calculations of wall shear stress and velocity profile in complex channels, considered two momentum terms in a manner similar to that presented by Hinze [9]. The first was a gradient transfer of momentum due to molecular friction and small-scale turbulent eddies. The second was a convective transfer of momentum due to large-scale motion of eddies. According to Ibragimov *et al.*, "the gradient transfer is determined by the local characteristics of the flow; however, the convective transfer depends mainly on the geometric features of the channel as a whole. In complex channels the effect of large-scale eddies on the velocity field should appear most strongly in the directions in which the velocity varies slowly (along the channel perimeter). Along the normal to a channel perimeter, however, convective transfer plays a small part since the velocity gradient is very high and hence so is the gradient of momentum. Convective transfer should appear more strongly in channels with a sharply

varying cross sectional shape (e.g. close-packed rods), when exchange between eddies of considerably different velocities may occur."

Subboten *et al.* [15], recently published experimental results that experimentally reinforce the concept of transverse macroscopic flow processes. They measured velocity profiles for air flowing in a pair of triangular pitch flow channels with p/d of 1·05, 1·10 and 1·20. Only for $p/d = 1{\cdot}05$ did the velocity profiles show distinct curvature of isovels (lines of constant velocity) due to the existence of secondary flows. This tends to be consistent with the ideas of Ibragimov because the shape varies more rapidly at $p/d = 1{\cdot}05$ than for p/d of 1·10 or 1·20.

Kjellström [16, 17] has reported what is believed to be the first results of rod-bundle turbulence measurements available in the open literature. He investigated the turbulent flow of air in an enlarged rod bundle of triangular array with a pitch-to-diameter ratio of 1·217 using a hot-wire anemometer. Secondary flows were measured; however, the velocities were less than 1 per cent of the axial velocity with considerable scatter in the data. The secondary flow pattern midway between the gap and subchannel center showed flow moving along the centerline toward the gap and away from the gap along the rod surface. The results of the turbulence measurements were used to calculate local eddy diffusivity. He found that the eddy diffusivity (momentum) is strongly nonisotropic—the diffusivity in the peripheral direction being a factor 5–1·5 higher than that in the radial direction. The higher value applies to the wall region and the lower one to the core of the flow.

These results suggest that secondary flows and possibly other macroscopic flow processes may exist in rod bundles in addition to the normally assumed eddy diffusion processes.

EDDY DIFFUSION ESTIMATES

An estimate of the eddy diffusion coefficient for scalar transport can be made in terms Lagrangian turbulence parameters using Taylor's analysis [18] as reported by Hinze [9]. For long diffusion times the eddy diffusion coefficient can be expressed as

$$\varepsilon = v' \Lambda_L; \tag{5}$$

the product of the Lagrangian lateral flow fluctuation and turbulence macroscale.

Classical mixing length theory may also be used. Following the approach of Welty *et al.* [19], the scalar transport may be expressed as

$$\overline{v'\gamma} = \overline{v'L}\frac{\partial \bar{\Gamma}}{\partial y} \tag{6}$$

where $\overline{v'L}$ is equivalent to the eddy diffusion coefficient. The product of intensity and the mixing length L is similar to the result obtained by Taylor. The mixing length represents the lateral distance travelled by the fluid packet associated with the fluctuating velocity v'. It could be expected that this length would also be of the same order but probably smaller than the size of longitudinal macroscale in the turbulent core away from the wall. If the suppositions of Ibragimov are correct, L could be larger in the circumferential direction than in the radial direction from the rod surface.

In the presence of macroscopic flow pulsations, Hinze [9] suggests

$$\overline{v'\gamma} = \varepsilon_\gamma \frac{\partial \bar{\Gamma}}{\partial y} + \overline{V'\gamma} \tag{7}$$

to account for macroscopic flows in the presence of eddy diffusion. The same equation has been suggested by Ibragimov [14] for rod bundles. By analogy to equation (6), $\overline{V'\gamma}$ may be expressed as

$$\overline{V'\gamma} = \overline{V'L}\frac{\partial \bar{\Gamma}}{\partial y}; \tag{8}$$

therefore

$$\overline{v'\gamma} = (\varepsilon_\gamma + \overline{V'L})\frac{\partial \bar{\Gamma}}{\partial y}. \tag{9}$$

The part of the scalar transport due to macroscopic pulsations is seen to add to that part due to conventional turbulent fluctuations by using mixing length theory. The total could also be thought of as an eddy diffusion coefficient but it would not necessarily correspond to an eddy diffusion coefficient for simple channels. Equation (9) contains the effects of flow channel geometry through the geometric effect on intensity and scale.

TURBULENCE PARAMETERS

The previous discussion points out that lateral Lagrangian velocity fluctuations and macroscale are fundamental parameters involved in the crossflow mixing processes. It would be very helpful to have a relationship between Eulerian and Lagrangian turbulence parameters. This would allow data from Eulerian experiments to be transferred to a Lagrangian description of the flow. Unfortunately not much is known about such relationships [9]. For homogeneous turbulence the value of v' could be set equal to the lateral component of turbulence velocity. In nonhomogeneous turbulence this would not be true but v' could be expected to be of the same order. Relationships between Λ_L and the longitudinal space macroscale Λ_f are believed to exist; but even for isotropic turbulence, such relationships apparently have not been found theoretically. According to Hinze [8], experimental evidence at large Reynolds numbers has shown that the Lagrangian correlation coefficient $R_L(\tau)$ and the longitudinal spatial correlation coefficient $f(r)$ are of similar

shape and can often be approximated by the exponential functions $\exp(-\tau/T_L)$ and $\exp(-r/\Lambda_f)$, respectively. Thus, if it is assumed that these correlations have the same functional form then the Lagrangian and Eulerian integral scales must be proportional.

Although the relationships between Lagrangian and Eulerian turbulence parameters are not complete, there does appear to be enough similarity that measurements of Eulerian macroscale and turbulence intensities could provide insight regarding rod bundle flow structure.

In this paper Taylor's hypothesis is used to obtain an estimate of the longitudinal macroscale defined by

$$\Lambda = uT_E \tag{10}$$

where the macro time scale is defined as

$$T_E = \int_0^\infty R_E(\tau)\,\mathrm{d}\tau \tag{11}$$

and the longitudinal Eulerian time correlation autocorrelation is defined by

$$R_E(\tau) = \frac{\overline{u'(t)u'(t-\tau)}}{\overline{u'^2}}. \tag{12}$$

Taylor's hypothesis can be justified if the flow field is homogeneous, if it has a constant mean velocity $\bar{u}$ in the x direction, and if $u' \ll \bar{u}$. These conditions are roughly approximated for rod bundle channel flow.

EXPERIMENTAL METHOD

An experimental study was performed to measure the velocity, turbulence intensity and Eulerian time macroscale at selected locations in rod bundle flow channels. The measurements were performed with a two-component laser–Doppler velocimeter. A complete description of the experimental set-up and instrumentation is presented in [20].

Laser–Doppler velocity measurement

The laser–Doppler velocity measurement technique uses the principle that coherent laser light scattered from a moving particle experiences a frequency shift. This phenomena, known as the Doppler shift, is detected by optical heterodyne mixing of the scattered light with the reference light from the same laser.

Several authors [21–23] have discussed derivation of the basic Doppler shift equation. The equation relating the Doppler shift to the velocity and geometry is given by

$$f_D = \frac{n}{\lambda_0} V \cdot (r_s - r_0) \tag{13}$$

where f_D is the Doppler shift frequency, V is the velocity vector, r_s is the unit vector for scattered light, r_0 is the unit vector for the reference light and λ_0 is the *in vacuo* wavelength of the laser light.

The turbulent velocity measurements were performed with a Laser Systems and Electronics two-component laser–Doppler velocimeter by using the optical arrangement shown in Fig. 1. The measured velocity components at $\pm 45°$ are resolved into the axial and lateral components u and v, respectively. One-component velocity measurements were obtained by using just one optical channel by rotating the optical unit 45°. The measurement point sample volume is estimated to be 0·026 in. (0·066 mm) long by 0·0034 in. (0·0086 mm) dia.

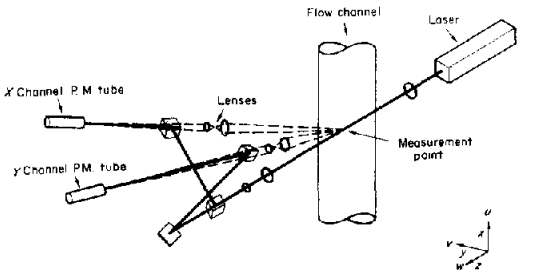

FIG. 1. Two-component laser–Doppler velocimeter optical arrangement.

Test section

Figure 2 shows a cross section view of the test section construction. It consisted of a front and back plate and flow housing body. The back plate contained the inlet and outlet nozzles and was permanently installed in the flow facility. The front plate was bolted to the back plate with the flow housing body placed between them. The 4 in. × 3¼ in. (10·16 cm × 8·26 cm) rectangular cavity dimensions were maintained by the restraining shoulder next to the "O-ring" groove on the front and back plates.

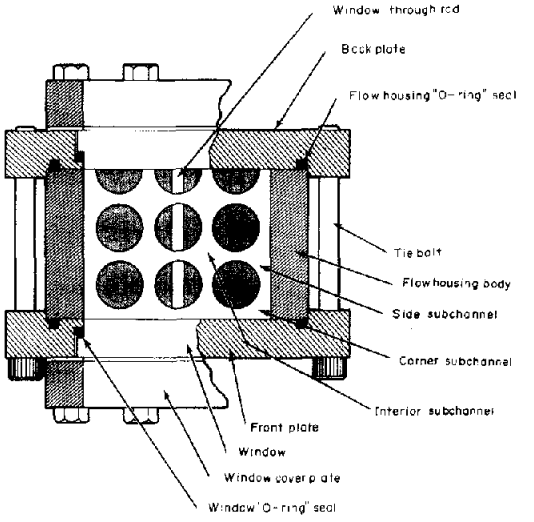

FIG. 2. Cross section view of flow model.

The front and back plates contained optically flat ($\lambda/4$) quartz windows 2 in. (5·08 cm) high for entrance and exit of the laser beam. A shim was placed between the window and cover plate to position the window "flush" with the inner surface of the flow housing.

All rods and sectors were 1 in. (2·54 cm) dia for $p/d = 1{\cdot}25$ and $1\frac{1}{8}$ in. (2·86 cm) dia for $p/d = 1{\cdot}125$. To maintain a clean geometry no spacing devices were used in the subchannels. The solid rods were supported at the ends only. Paint was applied to the rods to help reduce light reflections. Small windows were placed in the rods to allow the laser beam to pass through the rods. These windows and their rods had $\frac{1}{8}$ in. (3·18 mm) wide flats to eliminate distortion of the laser beam.

An 8 in. (20·3 cm) long flow straightening section was placed at the inlet of the flow channel. This consisted of four eccentric screens (60 per cent open) with $\frac{1}{4}$ in. (6·35 mm) holes in a triangular array followed by a bank of $\frac{1}{4}$ in. (6·35 mm) o.d., 0·020 in. (0·51 mm) wall tubes $3\frac{1}{2}$ in. (8·26 cm) long. The screens tended to equalize the inlet velocity distribution and the tubes helped to establish a fixed scale of turbulence and straighten the flow. The inlet ends of the rods and rod sectors had a 60° taper to minimize further disturbances of flow due to flow area change upon entering the rod section.

The exit from the rod section was an abrupt expansion to the plenum at the discharge nozzle. This was about 9 in. (22·9 cm) above the measurement plane which was over 75 equivalent diameters from the inlet of the bundle.

Turbulence signal processing

A Laser Systems and Electronics readout system was used to obtain values of average velocity and time varying fluctuating velocity component from the frequency modulated Doppler signal. The resulting fluctuating velocity analog signal was measured by first amplifying the signal, removing high-frequency Doppler ambiguity broadening by a low-pass filter and then measuring the true rms voltage. The voltage-to-Doppler conversion factor was determined for each observation from the slope of the f.m. detector characteristic. The fluctuating velocity signal was also fed into a Model 100 Princeton Applied Research signal correlator to compute the Eulerian time correlation (autocorrelation).

The autocorrelation function plots were fit to the equation

$$R(\tau) = e^{\alpha_1 \tau} \cos \alpha_2 \tau. \tag{14}$$

This was accomplished by dividing each plot into eleven equally spaced points and then fitting these points to equation (14) with a least squares curve fitting computer routine. By integrating according to equation (11), the scale estimate was defined as

$$\Lambda = \bar{u} T_E = \frac{\bar{u}\alpha_1}{\alpha_1^2 + \alpha_2^2}. \tag{15}$$

EXPERIMENTAL RESULTS

Velocity, turbulence intensity, and turbulence scale measurements were obtained at three Reynolds numbers, at various positions and for two values of rod gap spacing in the three rod bundle subchannel types identified in Fig. 2. Limited two-component data were also taken in an outer rod-wall gap and wall subchannel to determine the magnitude of the lateral component of intensity.

Maps of turbulence intensity

The map of the axial component turbulence intensity distributions in the side, corner, and interior subchannels are shown in Fig. 3. These data show some

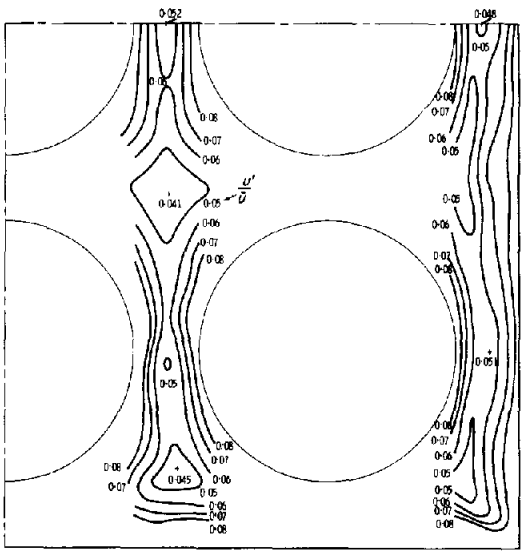

FIG. 3. Axial turbulence intensity distribution, $Re = 100000$, $p/d = 1{\cdot}25$.

new and interesting information regarding turbulence flow structure in rod bundles. An interesting feature is the relative minimum of turbulence intensity in the subchannel centers and rod gap centers. The minimum values of 0·041 and 0·045 in the center and wall subchannels are both higher than 0·035 which is typical for fully developed pipe flow [24–26]. The relative minima of 0·050 and 0·052 in the interior rod gaps are higher than the subchannel center values. Another interesting feature is the relative maximum† that occurs along the centerline between subchannel centers and

†This is actually a "saddle point" because the intensity increases toward the wall.

the gap. The corner and wall subchannel map show behavior similar to that found in the interior channel; however, it is modified by the presence of the flow housing wall. The relative minima and maxima are comparable to those in the interior.

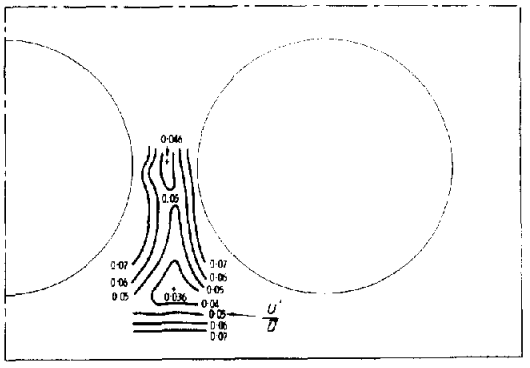

(a) Axial component intensity.

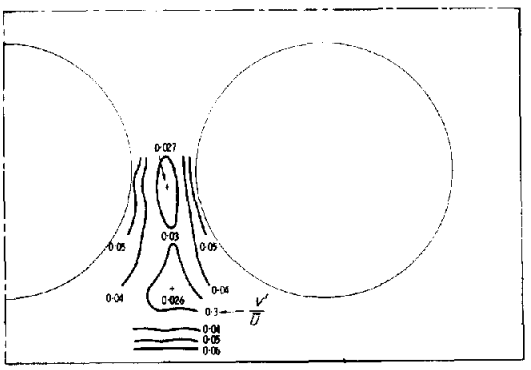

(b) Lateral component intensity.

FIG. 4. Axial and lateral turbulence intensity distribution, $Re = 100\,000$, $p/d = 1{\cdot}25$.

Figure 4 shows maps of turbulence intensity obtained in the axial and lateral directions within a wall subchannel. The axial component intensity distribution is very similar to that shown in Fig. 3; however, the values of intensity are about 10 per cent lower. The reason for this difference is believed to be caused by the lower turbulence cutoff frequency (3·0 kHz) as compared to the previous data (4·0 kHz). The lateral component of turbulence intensity is seen to be less than the axial component by about 40 per cent near the gap and about 30 per cent lower near the subchannel center. The lateral component near the wall is also lower by about 50 per cent. The gradients of the lateral component are also seen to be smaller in the interior part of the subchannel and gap. It should be noted that the lateral component is in the cartesian coordinate y direction indicated in Fig. 1.

One of the most obvious features of the intensity map is the distortions of the intensity distribution believed to be caused by secondary flows. Secondary flows are known to occur in the corner of square channels where a pair of secondary flow circuits move along the bisector of the corner angle toward the corner, along the channel wall and out into the main flow stream. These secondary flows also transport the properties of the flow such as the turbulence energy. In the corner subchannel of Fig. 3 a secondary flow moves toward the corner carrying lower intensity flow into the corner thus causing the intensity lines to "bulge" toward the corner. Likewise the return path carries high intensity wall turbulence toward the open part of the channel, thus causing a "bulge" away from the wall.

Examination of Fig. 3 indicates several other regions of possible secondary flow. Of particular importance are those that occur in regions between the rod gaps and subchannel centers. In general the secondary motion are not entirely consistent as indicated by the different intensity distortions in the various subchannels. It is interesting to note that the interior subchannels do not have the same shaped intensity distributions and there is incomplete symmetry about the lines of symmetry normally assumed with unit cell analyses.

Effect of Reynolds number

Figure 5 shows profiles of velocity, intensity, and scale along centerlines through rod gaps for Reynolds numbers of 50 000, 100 000 and 200 000. The lower value was obtained by reducing the flow by a factor of two at a given temperature and the higher value was obtained by increasing temperature to decrease the kinematic viscosity by a factor of two. The data in Fig. 5 shows very little change with Reynolds number at the $\frac{1}{4}$ in. (6·35 mm) gap spacing.

The plot of axial turbulence intensity ($u'/\bar{u}$) for the interior channel shows the relative minimum and maximum indicated by the previous intensity maps. The average value along the centerline of about 0·050 is somewhat higher than the value 0·035 that would be expected at the center of pipe flow. Figure 5 shows a rather uniform distribution of longitudinal turbulence scale. There is no evidence of significantly smaller scale in the gaps and larger scale in the subchannel. Figure 5(*b*) shows a more nonuniform distribution of scale along a line through the center of the wall rod-gaps. Although this is not a symmetric centerline traverse as in Fig. 5(*a*) the scale is of comparable magnitude. The corner subchannel shows somewhat smaller scale as compared to wall and interior subchannels. This could be expected because of the smaller subchannel hydraulic diameter as compared to the bundle average value. The scale in the gap between the corner and wall subchannel is about one-half that in the side subchannel. The scale in the gap between the side-wall channels is only a little smaller than the scale in the

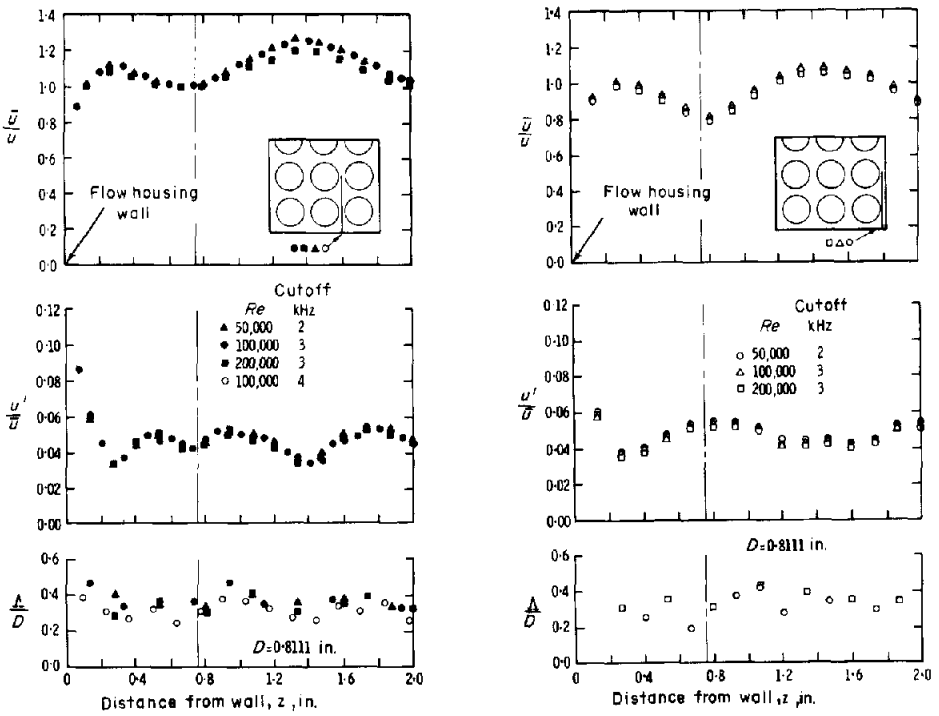

(a) Wall and interior channel. (b) Corner and wall channel.

FIG. 5. Axial velocity, turbulence intensity, and macroscale along gap centerline traverse, $\frac{1}{4}$ in. gap spacing.

wall subchannels. The general result is that the scale is rather uniform with moderately reduced values in some gaps. The longitudinal scale is generally 0·3–0·4 times the hydraulic diameter.

Effect of rod gap spacing

The effect of rod gap spacing on the velocity, intensity, and scale was investigated by increasing the rod diameter from 1 in. (2·54 cm) to $1\frac{1}{8}$ in. (2·86 cm). This decreased the center rod gap spacing from $\frac{1}{4}$ in. (6·35 mm) to $\frac{1}{8}$ in. (3·18 mm) and decreased the side wall gap spacing from $\frac{1}{4}$ in. (6·35 mm) to $\frac{3}{16}$ in. (4·76 mm). The results in Fig. 6 confirm the weak Reynolds number effect found at the larger gap spacing. A comparison of Figs. 5 and 6 show, however, that the reduced gap spacing significantly increases the intensity and modifies the scale distribution, especially near the rod gap. As for the larger spacing, a relative minimum in intensity occurs near the subchannel center and the center of the rod gap. The average intensity is about 60 per cent higher along the interior channel centerline for the $\frac{1}{8}$ in. (3·18 mm) gap spacing as compared to the $\frac{1}{4}$ in. (6·35 mm) gap spacing. Most of this increase is due to significantly higher intensity on each side of the gap. The gap intensity is also higher but less than the adjacent peak values. The data also show a significantly modified distribution and a general increase of scale in the wall and interior subchannel at the reduced gap spacing. Maximum and minimum values of $\Lambda/D = 0{\cdot}70$ and 0·25 correspond to values of $\Lambda = 0{\cdot}57$ in. (1·45 mm) and 0·20 in. (0·51 mm) respectively. This magnitude of scale as compared to the $\frac{1}{8}$ in. (0·318 mm) gap spacing indicates elongated eddies in the axial and probably in the lateral direction through the gap.

The distribution of scale for the $\frac{1}{8}$ in. (0·318 mm) interior gap is rather interesting because the largest scales are in the rod gap and at the subchannel centers. The smaller scale turbulence is located between the gap and subchannel center. The correlation functions also show this to be a region of significant periodic flow pulsation; whereas, no significant flow pulsations are indicated in the data at the larger gap spacing.

The results for the corner and wall subchannels shown in Fig. 6(*b*) are quite different. The intensity data do not show an increase but a decrease for the reduced gap spacing to $\frac{3}{16}$ in. (0·476 mm). The longitudinal scale, however, shows nearly a factor of two increase for the reduced spacing. The scale is a little smaller in the gap as compared to the scale in the subchannel. Maximum and minimum values of $\Lambda/D = 0{\cdot}78$ and 0·40 correspond to values of $\Lambda = 0{\cdot}60$ in. (1·52 mm) and 0·30 in. (0·762 mm), respectively, for the $\frac{3}{16}$ in. (0·476 mm) wall gap spacing.

The different behavior between interior and wall subchannels suggests a subchannel shape effect on intersubchannel mixing. Additional data [20] show

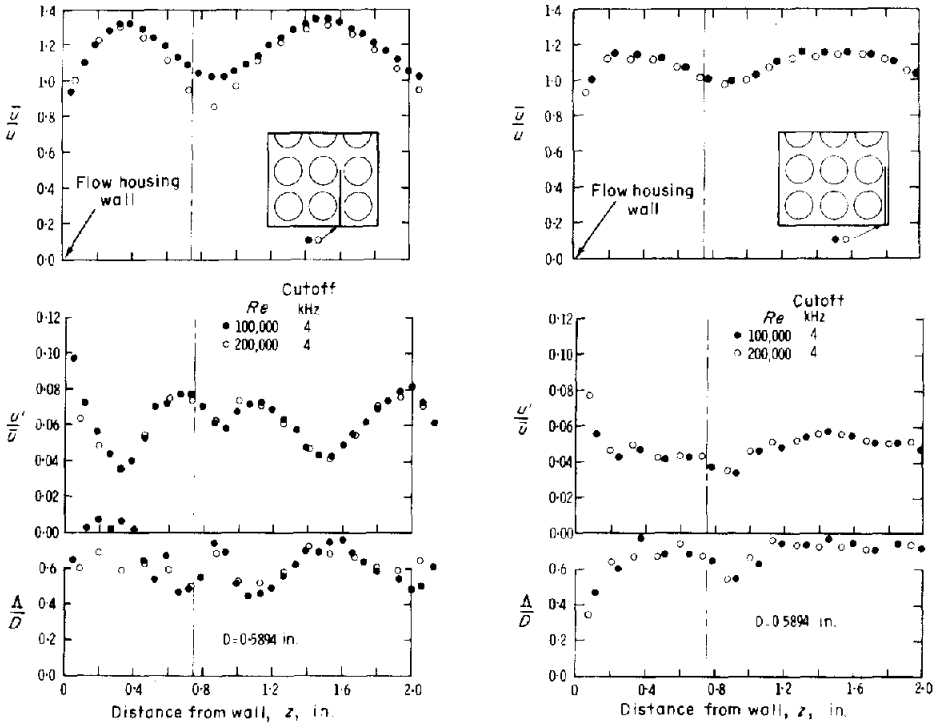

(a) Wall and interior channel. (b) Corner and wall channel.

FIG. 6. Axial velocity, turbulence intensity, and macroscale along gap centerline traverse, $\frac{1}{8}$ in. internal gap, $\frac{3}{16}$ in. wall gap.

that different shape adjacent subchannels do not significantly affect the flow structure near the rod gap; however, all of those subchannels had symmetry about the centerline through the gap. The wall subchannels are different in that they do not have the same symmetry.

Flow structure in rod gap

Since there has been considerable interest and speculation concerning turbulent flow structure in the rod gaps of rod bundles, considerable experimental effort was directed toward investigating that region.

Figure 7 presents a comparison of the rod gap turbulence intensity data with the results of Kjellström [16, 17] for rod bundles and Laufer [24] for round tubes normalized to the shear velocity.†

Figures 7(*a*) and 7(*b*) present two-component data obtained in rod-wall gaps. The agreement is quite good; however, there is indication of lower axial component intensity near the walls.

Figure 7(*c*) presents turbulence intensity data obtained in the side rod-wall gaps and interior rod-rod gaps. These data show about the same average values as the data of Kjellström and Laufer; however, the distributions are significantly different. The intensity map of Fig. 3 suggests that secondary flows could exist in, or near, these rod gaps. Secondary flows carrying turbulence from the wall or subchannel interior into the rod gap could produce the observed redistribution effects.

Comparison of the data in Fig. 7(*c*) with the data in Figs. 7(*a*) and 7(*b*) show the difference depends on the orientation of the wall. In Fig. 7(*c*) the wall was parallel with the laser beam and was smooth over its entire length. The front wall, however, was normal to the laser beam but contained four additional window ports located at one foot intervals below the measurement window. Each window plug was flush with the inner surface of the flow housing wall but very small slots approximately 0·010 in. wide and full width existed at the leading and trailing edge of each window port plug. These slots could have modified the boundary layer and secondary flow development along the wall so as to reduce the effect of secondary flows on the turbulence in the gaps.

DISCUSSION OF RESULTS

Macroscale and correlation functions

It is well known that the Fourier cosine transform of the autocorrelation function gives the power spectrum of turbulence energy. If the correlation function exhibits periodic behavior with an exponential decay,

†$U/U^* = \sqrt{f/8}$ where $f = 0{\cdot}157\,Re^{-0{\cdot}187}$ based on channel pressure drop measurements.

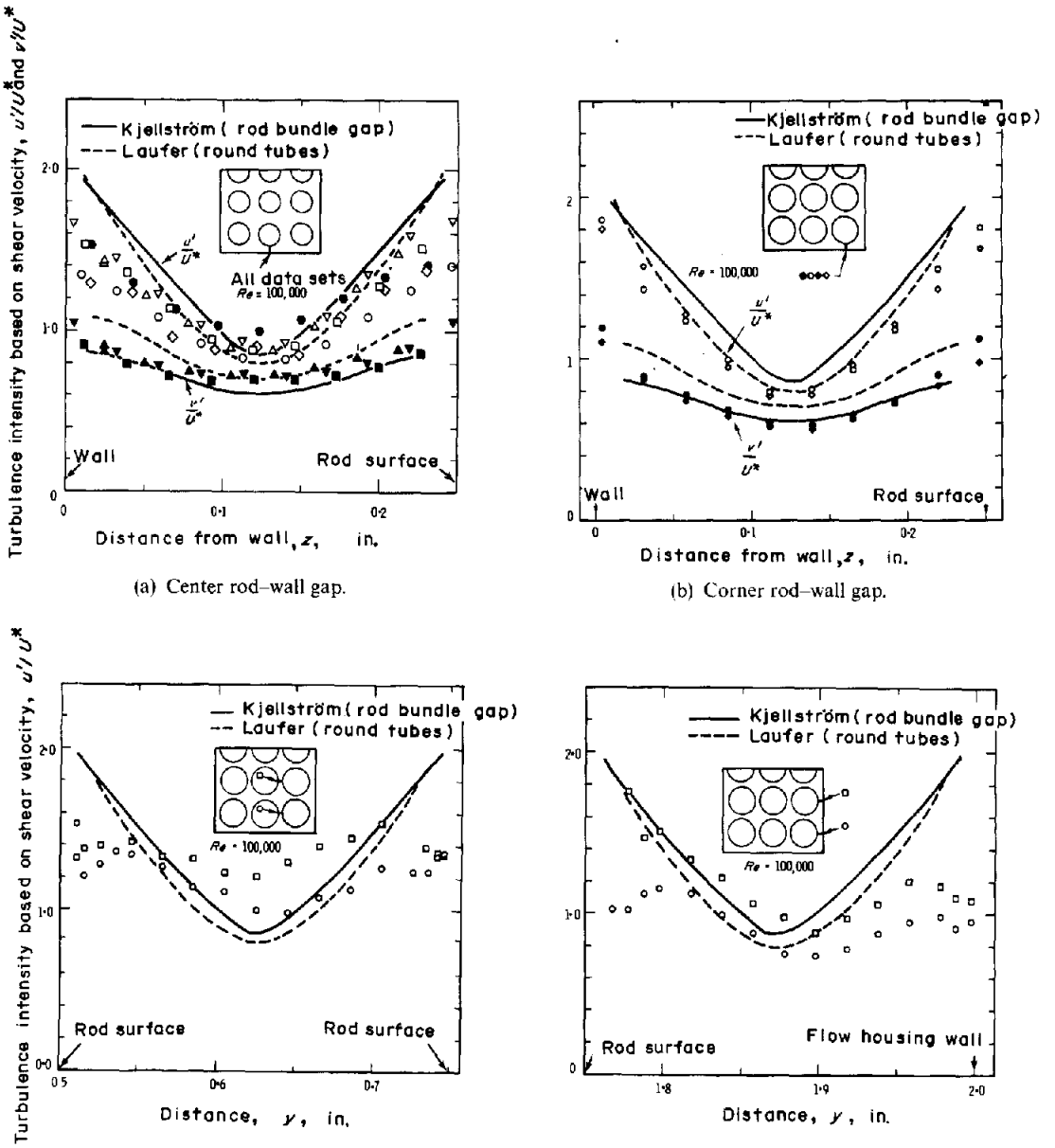

(a) Center rod–wall gap.

(b) Corner rod–wall gap.

(c) Interior rod–wall gap.

(d) Side rod–wall gap.

FIG. 7. Comparison of gap turbulence intensity data with the data of Laufer and Kjellström.

the power spectrum has a peak at a frequency corresponding to the dominant frequency of correlation function. Periodic behavior shown by the correlation function, therefore, indicates a dominant frequency in the power spectrum. The relative importance of a dominant periodic component can be judged rather quickly by just inspecting the autocorrelation function.

Most of the measured autocorrelation functions in this study had nearly an exponential decay with little or no evidence of dominant periodic behavior; however, some of the autocorrelation functions obtained in certain regions of the flow channel at the smaller rod gap spacing did show definite periodic behavior. These were limited to the region between the subchannel center and rod gap where there was also evidence of secondary flows.

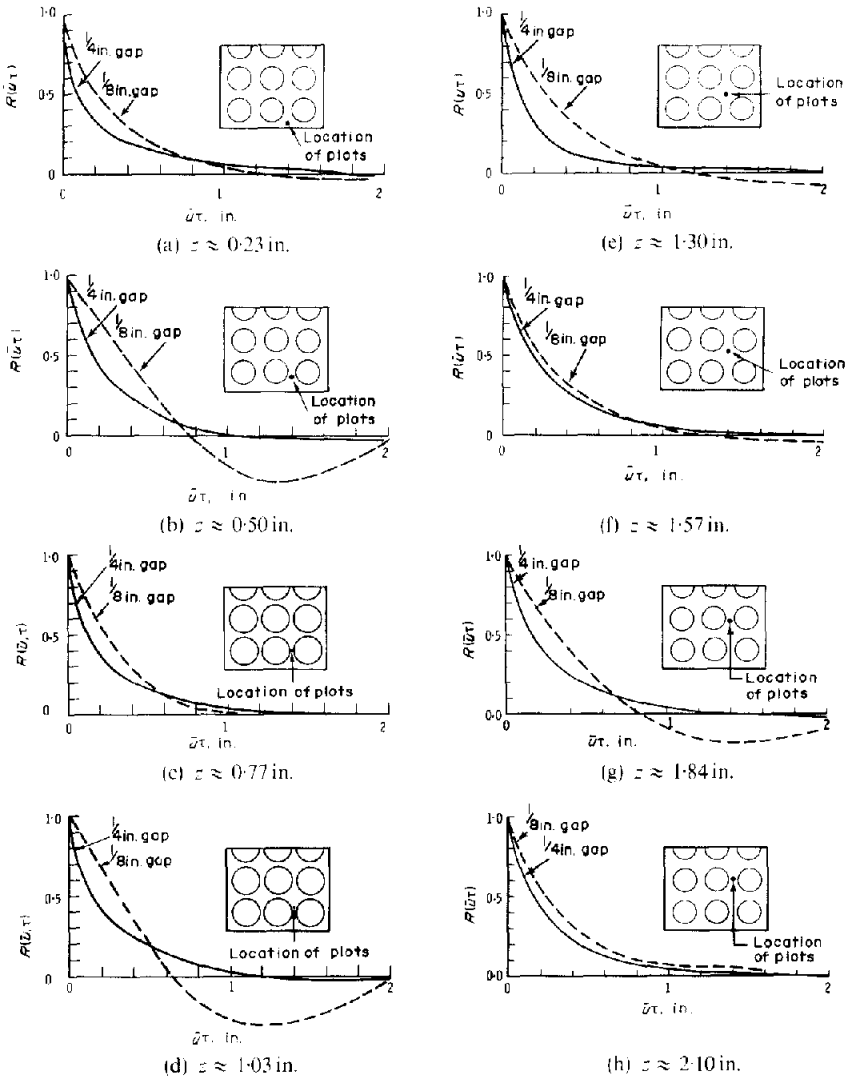

FIG. 8. Autocorrelation plots at selected locations in subchannels, $Re = 10\,000$.

Figure 8 shows autocorrelation functions obtained along the interior subchannel centerline at a Reynolds number of 100 000 for the two gap spacings. There is a definite change in the autocorrelation function with distance from the wall and on through the gap into the interior subchannel. Near the flow housing wall, subchannel center and in the rod gap the autocorrelation function is nearly exponential. Here the macroscale estimate depends primarily on the decay of the autocorrelation function. In the region between the gap and subchannel center, the correlation function at the smaller gap spacing shows periodic behavior. Here the macroscale estimate also depends on the frequency of the autocorrelation function as shown by equation (15).

Figure 9 shows a plot of the frequency distribution along the centerline through the rod gaps. It shows regions of dominant periodic motion between the rod gap and subchannel center for the smaller gap spacing.

From these experimental results it can be concluded that the reduction of rod gap spacing leads to more dominant periodic flow pulsations in the regions adjacent to the rod gap. This together with secondary flows, increased turbulence intensity and increased macroscale indicate an enhancement of crossflow mixing to help compensate for a decrease in rod gap spacing.

Implications regarding crossflow mixing

The experimental data show that significant variations of intensity and scale can occur with changes in rod bundle geometry and that macroscopic flow processes contribute to ε/UD in regions adjacent to the rod gaps.

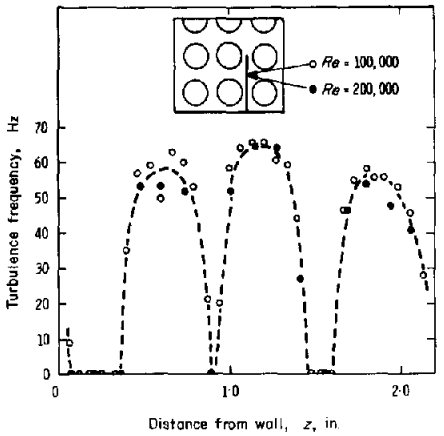

FIG. 9. Dominant turbulence frequency as estimated from autocorrelation function data.

Referring to equation (5), an estimate of the parameter ε/UD could be expressed as the ratios

$$\frac{\varepsilon}{UD} = \left(\frac{u'}{\bar{u}}\right)\left(\frac{\bar{u}}{U}\right)\left(\frac{\Lambda}{D}\right)\left(\frac{\Lambda_L}{\Lambda}\right)\left(\frac{v'}{u'}\right). \tag{16}$$

The first three parameters are those measured in this study. The last two are the ratios required to convert from an Eulerian to a Lagrangian representation of lateral scalar transport. For homogeneous turbulence the value of v' would be of the same magnitude as the lateral component of turbulence velocity. Based on the measurements in this study the ratio v'/u' would be less than unity and could have values in the range from about 0·5 to 0·8. The Lagrangian macroscale [1,8] could be expected to be of the same order of magnitude as the lateral macroscale of turbulence which would be less than the longitudinal macroscale measured in this study. An estimate for ε/UD could be written as

$$\frac{\varepsilon}{UD} \propto \left(\frac{u'}{\bar{u}}\right)\left(\frac{\bar{u}}{U}\right)\left(\frac{\Lambda}{D}\right) \tag{17}$$

where the proportionality factor would be less than unity and with uncertain functional variation with geometry and flow conditions.

The present data are not complete enough to determine channel average values for the above parameters; however, from the centerline traverses, some estimates can be obtained to give an indication of how the parameters change with geometry. The summary estimates in Table 1 show an increase in $(u'/U)(\Lambda/D)$ that varies inversely with the gap spacing. The change is primarily due to an increase in macroscale with a decrease in gap spacing. This macroscale increase is interesting because the scale in round pipes would vary with pipe diameter. The present data indicate that scale cannot be estimated from channel size alone.

Table 1. Representative average estimates of turbulence parameters along traverse centerlines

Gap spacing (in.)	$\frac{u'}{U}$	$\frac{\Lambda}{D}$	$\frac{s}{\Delta y}$	$\left(\frac{u'}{U}\right)\left(\frac{\Lambda}{D}\right)$	$\frac{u}{U}\frac{\Lambda}{D}\frac{s}{\Delta y}$
Interior subchannels					
$\frac{1}{4}$	0·050	0·35	0·20	0·018	0·0035
$\frac{1}{8}$	0·060	0·60	0·10	0·036	0·0036
Wall subchannels					
$\frac{1}{4}$	0·060	0·35	0·20	0·021	0·0042
$\frac{3}{16}$	0·050	0·70	0·15	0·035	0·0052
Corner subchannels					
$\frac{1}{4}$	0·055	0·30	0·22	0·017	0·0037
$\frac{3}{16}$	0·045	0·60	0·17	0·027	0·0046

The macroscale estimates presented here are for the longitudinal direction. It is probable that the scale is smaller in the lateral directions. While the scale may be restricted in size in the direction perpendicular to the wall, the scale in the direction parallel to the wall may not be so restricted. The present data suggests that the lateral freedom of the open array allows rather large scale turbulence to move through the gap with relative ease. This is consistent with the ideas of Ibragimov *et al.*, involving the motion of large scale eddies being felt most strongly along the perimeter of a channel with a sharply varying cross sectional shape, such as a rod bundle. As the gap becomes very small such turbulent motion could not penetrate the gap because of the dominance of the laminar boundary layer. Galbraith found a significant reduction in crossflow mixing when rod gap was reduced from 0·028 in. (0·071 mm) to 0·011 in. (0·028 mm) when using 1 in. (2·54 cm) diameter rods.

The changes of $(u'/U)(\Lambda/D)$ shown in Table 1 are nearly inversely proportional to gap spacing and taken together with the ratio $s/\Delta y$ yield an estimate for w'/GD that is relatively constant. This result together with the weak effect of Reynolds number of the turbulence parameters is consistent with the predicted trends of present crossflow mixing correlations. This is a significant result because it helps to explain why crossflow mixing in bundles is weakly dependent on rod spacing over a rather wide range of sufficiently large spacings.

The direct measurement of the turbulence parameters related to the crossflow mixing processes also provides additional insight concerning the physical processes of crossflow mixing. The experimental data indicate that the regions adjacent to the rod gaps have flow processes that are both diffusive and convective; whereas, the subchannel center and rod gaps are more nearly diffusive. The data also indicate that the eddy diffusion estimates cannot be predicted from pipe data alone.

Thus the eddy diffusion in bundles is augmented by macroscopic flow processes. This result supports the earlier contentions of Rowe [27], Skinner *et al.* [13], and Ibragimov [14] that macroscopic flow processes in addition to eddy diffusion are involved in the lateral mixing processes in rod bundles.

REFERENCES

1. R. W. Bowring, HAMBO: A computer program for the subchannel analysis of the hydraulic and burnout characteristics of rod clusters, Atomic Energy Establishment, AEEW-R-582 (1968).
2. J. T. Rogers and N. E. Todreas, Coolant interchannel mixing in reactor fuel rod bundles, single-phase coolants, *Heat Transfer in Rod Bundles*, pp. 1–56. American Society of Mechanical Engineers (1968).
3. D. S. Rowe, A thermal-hydraulic subchannel analysis for rod bundle nuclear fuel elements, *Heat Transfer 1970*, Vol. 3, FC 7.11 (1970).
4. D. S. Rowe, COBRA-IIIC: A digital computer program for thermal-hydraulic subchannel analysis of rod bundle nuclear fuel elements, Battelle Memorial Institute, Pacific Northwest Laboratories, BNWL-1695, 55p (1973).
5. K. P. Galbraith, Single phase turbulent mixing between adjacent channels in rod bundles, Ph.D. Thesis, Corvallis, Oregon, Oregon State University (June, 1971).
6. K. P. Galbraith and J. G. Knudsen, Turbulent mixing between adjacent channels for single phase flow in a rod bundle. American Institute of Chemical Engineers, Preprint 19 (1971).
7. L. Ingesson and S. Hedberg, Heat transfer between subchannels in a rod bundle, *Heat Transfer 1970*, Vol. 3, FC 7.11 (1970).
8. J. T. Rogers and R. G. Rosehart, Mixing by turbulent interchange in fuel bundles, correlations and inferences, ASME paper no. 72-HT-53 (1972).
9. J. O. Hinze, *Turbulence*. McGraw-Hill, New York (1959).
10. A. C. Rapier, Turbulent mixing in a fluid flowing in a passage of constant cross section, United Kingdom Atomic Energy Authority, Reactor Development Laboratory, Windscale, Great Britain. TGR Report 1417(W) (1967).
11. D. S. Rowe and C. W. Angle, Cross-flow mixing between parallel flow channels during boiling. Part II. Measurement of flow and enthalpy in two parallel channels, Battelle Memorial Institute, Pacific Northwest Laboratories, BNWL-371-PTII (1967).
12. D. S. Rowe and C. W. Angle, Cross-flow mixing between parallel flow channels during boiling. Part III. Effect of spacers on mixing between channels. Battelle Memorial Institute, Pacific Northwest Laboratories, BNWL-371-PTIII (1968).
13. J. R. Skinner, A. R. Freeman and H. G. Lyall, Gas mixing in rod clusters, *Int. J. Heat Mass Transfer* **12**, 265–278 (1969).
14. M. Kh. Ibragimov, I. A. Isupov, L. L. Kobzar and V. I. Subbotin, Calculation of the tangential stresses at the wall in a channel and the velocity distribution in a turbulent flow of liquid, *Atomic Energy* **21**, 731–739 (1966).
15. V. I. Subbotin, P. A. Ushakov, Yu. D. Levchenko and A. M. Aleksandrov, Velocity fields in turbulent flow past rod bundles. *Heat Transfer—Soviet Research* **3**, 9–35 (1971).
16. B. Kjellström, Studies of turbulent flow parallel to a rod bundle of triangular array, AB Atomenergi, Studsvik, 611 01 Nyköping, Sweden, STU 68-263/u210 (1971).
17. B. Kjellström, Transport processes in turbulent channel flow, AB Atomenergi, Studsvik, 611 01 Nyköping, Sweden, STU project 70-409/u340 (final report), AE-RL-1344 (1972).
18. G. I. Taylor, Statistical theory of turbulence, *Proc. R. Soc., Lond.* **151A**, 421–478 (1935).
19. J. R. Welty, C. E. Wicks and R. E. Wilson, *Fundamentals of Momentum, Heat and Mass Transfer*. Wiley, New York (1969).
20. D. S. Rowe, Measurement of turbulent velocity, intensity and scale in rod bundle flow channels, Ph.D. Thesis, Corvallis, Oregon, Oregon State University (June 1973). (Available as USAEC document BNWL-1736.)
21. W. K. George, An analysis of the laser–Doppler velocimeter and its application to the measurement of turbulence, Ph.D. Thesis, Baltimore, Maryland, The Johns Hopkins University (1971).
22. L. Lading, Differential Doppler heterodyning technique, *Appl. Optics* **10**, 1943–1949 (1971).
23. Y. Yeh and H. Z. Cummins, Localized fluid flow measurements with a He–Ne laser spectrometer, *Appl. Phys. Lett.* **4**, 176–178 (1964).
24. J. Laufer, The structure of turbulence in fully developed pipe flow, National Advisory Committee for Aeronautics, NACA-TN-2954 (1953).
25. K. Rehme, Untersuchungen der turbulenz—und schubspannungsverteilung an einem kreisrohr mit einem Hitzdraht-Anemometer, Gesellschaft für Kernfarschung mbH., Karlsruhe. KFK-1642 (1972).
26. L. V. Baldwin and T. J. Walsh, Turbulent diffusion in the core of fully developed pipe flow, *A.I.Ch.E. Jl* **7**, 53–61 (1961).
27. D. S. Rowe, A mechanism for turbulent mixing between rod bundle subchannels. *Trans. Am. Nucl. Soc.* **12**, 805 (1969).

ETUDE EXPERIMENTALE SUR LA STRUCTURE TURBULENTE DE L'ECOULEMENT ET MELANGE TRANSVERSAL DANS UNE GRAPPE DE BARREAUX

Résumé Une recherche expérimentale est menée sur l'effet de la géométrie du canal sur l'écoulement turbulent entièrement développé dans les canaux d'une grappe de barreaux. Cette information a été recherchée afin d'obtenir une meilleure compréhension du mélange transversal entre les sous-canaux d'une grappe de barreaux. Les expériences ont été faites avec l'eau pour un domaine du nombre de Reynolds allant de 50 000 à 200 000. Les modèles d'écoulement expérimentaux considèrent des rapports du pas au diamètre de 1,25 et 1,125. Les mesures principales sont celles des composantes axiales de la

vitesse, de l'intensité de turbulence et de la fonction d'autocorrélation eulérienne. La fonction d'autocorrélation donne une indication de la fréquence dominante de turbulence et une estimation de la macro-échelle longitudinale à l'aide de l'hypothèse de Taylor. Des résultats fragmentaires sur l'intensité de turbulence relative à la composante latérale ont été aussi obtenus.

Les résultats expérimentaux montrent que l'espace entre les barres (rapport du pas au diamètre) est le paramètre géométrique le plus influent sur la structure d'écoulement. La diminution de l'espacement entre barreaux accroit l'intensité de turbulence, la macro échelle longitudinale, et la fréquence dominante de turbulence. Ces paramètres de turbulence sont à peu près indépendants du nombre de Reynolds.

Les résultats indiquent que les processus macroscopiques d'écoulement sont liés à l'espacement des barreaux. Cela concerne les écoulements secondaires et l'accroissement du niveau et de la fréquence des pulsations de l'écoulement quand l'espacement est réduit. Interprêtés en rapport avec le mélange transversal. Les résultats sont en liaison étroite avec celui-ci.

KREUZSTROMQUERVERMISCHUNG AUFGRUND VON MESSUNGEN DER TURBULENTEN STRÖMUNGSSTRUKTUR

Zusammenfassung—Experimentell wurde der Einfluß der Kanalgeometrie bei voll turbulenter Strömung in einem Stabbündel-Strömungskanal untersucht. Diese Information sollte ein besseres Verständnis der Vermischung bei Kreuzstrom zwischen den Stabbündelkanälen liefern. Die Versuche wurden in Wasser in einem Bereich von Reynolds-Zahlen 50000 bis 200000 durchgeführt. Die experimentellen Strömungsmodelle berücksichtigten ein Längen-Durchmesserverhältnis von 1,25 und 1,125. Axialkomponenten der Geschwindigkeit, der Turbulenz-Intensität und der Eulerschen Autokorrelationsfunktion waren vorherrschende Messergebnisse. Die Autokorrelationsfunktion lieferte einen Hinweis auf die dominante Turbulenz-Frequenz und eine Abschätzung der longitudinalen Größenordnung bei Verwendung der Taylorschen Hypothese. Eine begrenzte Datenmenge der Seitenkomponente der Turbulenzintensität wurde ebenfalls erhalten. Die experimentellen Ergebnisse zeigen, daß die Spaltweite (Teilung-zu-Durchmesserverhältnis) der zutreffendste geometrische Parameter für die Strömungsstruktur ist. Bei abnehmender Spaltweite nehmen die Turbulenzintensität, die longitudinale Größenordnung und die dominante Turbulenzfrequenz zu. Diese Turbulenz-Parameter sind von der Reynolds-Zahl weitgehend unabhängig.

Die Ergebnisse zeigen, daß makroskopische Strömungsverläufe nahe dem Stabspalt existieren. Dies schließt Sekundärströmungen und zunehmende Frequenzen der Strömungspulsation ein bei abnehmender Spaltweite. Bei Darstellung mit Ausdrücken für Kreuzstrommischung stimmen die Ergebnisse mit bekannten Korrelationen überein.

ИНФОРМАЦИЯ О ЯВЛЕНИЯХ ПЕРЕМЕШИВАНИЯ ПРИ ОБТЕКАНИИ ПУЧКА СТЕРЖНЕЙ, ПОЛУЧЕННАЯ НА ОСНОВЕ ИЗМЕРЕНИЙ СТРУКТУРЫ ТУРБУЛЕНТНОГО ТЕЧЕНИЯ

Аннотация — Проведено экспериментальное исследование влияния геометрии на полностью развитое течение в свободных ячейках пучков стержней при их поперечном обтекании. Эта информация необходима для лучшего понимания процесса смешения турбулентной жидкости из разных ячеек пучка стержней. Опыты проводились с водой в диапазоне чисел Рейнольдса от 50 000 до 200 000. В экспериментальных моделях течения использовались отношения шага к диаметру, равные 1,25 и 1,125. Исходными экспериментально определяемыми величинами были осевые компоненты скорости, интенсивность турбулентности и эйлерова функция автокорреляции. С помощью функции автокорреляции определялась характерная частота турбулентности, и с помощью гипотезы Тейлора определялся продольный макромасштаб. Получены также некоторые данные о боковой компоненте интенсивности турбулентности. Экспериментальные данные показывают, что расстояние между стержнями (отношение шага к диаметру) является геометрическим параметром, определяющим структуру потока. С уменьшением расстояния между стержнями увеличивается интенсивность турбулентности, продольный макромасштаб и характерная частота турбулентности. Эти параметры зависят от чисел Рейнольдса. Результаты показывают, что в области, примыкающей к зазору между стержнями, имеют место макроскопические гидродинамические процессы, такие как вторичные течения, и увеличение масштаба и характерной частоты пульсаций течения при уменьшении зазора.